

EUROPEAN ORGANIZATION FOR NUCLEAR RESEARCH

CERN - SL DIVISION

CERN-SL-2000-058 AP

CLIC Note 447

DESIGN STATUS OF THE CLIC 3-TEV BEAM DELIVERY SYSTEM AND DAMPING RINGS

R. Assmann, H. Burkhardt, S. Fartoukh, J.B. Jeanneret,
J.M. Jowett, A. H. Owen*, O. Napoly**, F. Ruggiero,
D. Schulte, A. Verdier, L. Vos, E. Wildner, F. Zimmermann,

Abstract

We describe the present design status of beam delivery and damping rings for CLIC at 3 TeV cm energy, and outline our future plans. The beam delivery system comprises collimation, final focus and post-IP exit line. Critical design aspects include halo collimation, machine protection, beam removal, and thermal stability analysis. In order to attain the design spot size at the collision point, the damping rings must provide beams of extremely small emittances. In this paper, we focus on collimation and spent beam.

Paper presented at EPAC2000, 26-30 June 2000, Vienna, Austria

* CLRC,

**CEA Saclay

Geneva, Switzerland

08.08.00

DESIGN STATUS OF THE CLIC 3-TEV BEAM DELIVERY SYSTEM AND DAMPING RINGS

R. Assmann, H. Burkhardt, S. Fartoukh, J.B. Jeanneret, J.M. Jowett, F. Ruggiero, D. Schulte, A. Verdier, L. Vos, E. Wildner, F. Zimmermann, CERN, H. Owen, CLRC, O. Napoly, CEA/Saclay

Abstract

We describe the present design status of beam delivery and damping rings for CLIC at 3 TeV cm energy, and outline our future plans. The beam delivery system comprises collimation, final focus and post-IP exit line. Critical design aspects include halo collimation, machine protection, beam removal, and thermal stability analysis. In order to attain the design spot size at the collision point, the damping rings must provide beams of extremely small emittances. In this paper, we focus on collimation and spent beam.

1 BEAM DELIVERY

The beam delivery system encompasses collimation, final focus, interaction-point (IP) region, and exit line. A 3.3-km long base-line final-focus optics for 3 TeV is described in a companion paper [1]. We are presently exploring shorter alternatives either using dispersion across the final doublet, as proposed by Raimondi [2], or using microwave quadrupoles, proposed by Fartoukh and Jeanneret [3]. Ref. [4] compares stability issues for CLIC with those for other linear colliders. Here, we report on collimation and spent beam.

The collimation system should (1) remove the beam halo which otherwise would cause unacceptable background in the particle-physics detector, and (2) protect the downstream systems against the impact of a mis-steered beam. Point (1) is achieved if the collimator shadows the final doublet apertures on the incoming side from the impact of beam particles or synchrotron radiation. To this end, the collimation aperture should be less than $\pm 25 \sigma_x$ horizontally and $\pm 80 \sigma_y$ vertically [5], assuming the final quadrupole is a permanent magnet with 3.3 mm aperture, or 400 σ_x and 1000 σ_y for a superconducting final quadrupole with large bore. The apertures on the outgoing side need not be shadowed by the collimation, since the incoming halo is tiny compared with the wide-angle debris and beamstrahlung coming from the collision point [6]. By the same argument, background from synchrotron radiation emitted in the final quadrupoles is expected to be insignificant, as long as it does not hit apertures on the incoming side.

If a first beam halo collimation is performed prior to injection into the main linac, the halo at the entrance to the final focus, due to all known scattering sources, is estimated to be of the order of only 10^2 or 10^4 particles per bunch [7, 8]. Thus it appears that the collimators could be installed in the final focus itself, still retaining a tolerable detector background. For example, one muon is generated

at the collimator for every few 10^4 scraped particles, while it is likely that hundred muons passing through the detector per bunch train are acceptable [9]. The above numbers imply a few orders of magnitude safety margin for the muon background, if the final-focus collimation is performed 1 or 2 km upstream of the IP, and assuming that only a small fraction of the muons produced there will reach the detector. Collimation in the final focus does not only shorten the overall system length, but, in addition, we can profit from the naturally large beta functions in this region. Also non-linear collimation systems à la KEK [10] or TESLA [11] could be integrated into the final focus, *e.g.*, utilizing the sextupoles in the two chromatic correction sections. Note that up to a few percent of the beam had to be collimated at the end of the SLC linac. We assume that a pre-linac collimation will avoid a similar situation.

In order that the collimators are not destroyed by surface cracking during the impact of one bunch train, the lower limit on the beam size at the collimator is [12]:

$$\sigma_x \sigma_y > \frac{\alpha Y}{\sigma_{\text{UTS}} c_p} \frac{dE}{dx} \frac{N_b n_b}{2\pi} \quad (1)$$

where σ_{UTS} denotes the ultimate tensile strength, α the linear thermal expansion coefficient, c_p the heat capacity per unit density, Y the elastic modulus, dE/dx the ionisation energy loss per unit length, n_b the number of bunches per train, and N_b the bunch population. Table 1 lists example parameters for various materials and the minimum spot size $\sigma_{\text{min}} = \sqrt{\sigma_x \sigma_y}$ according to Eq. (1). For copper, we

Table 1: Physical properties of various materials and minimum beam size required for collimator survival.

mat.	α [$10^{-6}/\text{K}$]	Y [GPa]	c_p [$\frac{\text{MJ}}{\text{m}^3\text{K}}$]	K [$\frac{\text{W}}{\text{Km}}$]
Cu	16.5	120	3.4	390
Ti	8.5	110	2.4	17
W	4.4	411	2.5	200

mat.	σ [$\Omega^{-1}\text{m}^{-1}$]	dE/dx [10^{-10} J/m]	σ_{UTS} [MPa]	σ_{min} [μm]
Cu	6×10^7	2.1	300	200
Ti	2×10^6	1.1	400	100
W	2×10^7	3.6	350	270

find $\sqrt{\sigma_x \sigma_y} > 200 \mu\text{m}$ or $\sqrt{\beta_x \beta_y} \geq 1000 \text{ km}$, and, for titanium, $\sqrt{\sigma_x \sigma_y} > 100 \mu\text{m}$. In our present final-focus design, the maximum spot sizes for nominal beam param-

eters are $\sqrt{\sigma_x\sigma_y} \approx 45\mu\text{m}$ at the first three sextupoles, and $\sqrt{\sigma_x\sigma_y} \approx 76\mu\text{m}$ at the last one. These numbers are close to the required minimum. Materials with a smaller product αE would be better suited for collimation. We are contemplating the use of carbon composites [13]. Further work includes the computation of time-dependent temperature along a batch in order to determine meltings limits, and the study of active protection schemes with risk analysis.

Also image currents can heat the collimator surface. Table 2 lists the maximum rise in surface temperature during the passage of a single bunch, ΔT_1 or a full bunch train, ΔT_N , using the formulae derived in Ref. [14] and assuming a spot size $(\sigma_x\sigma_y)^{1/2} \approx 50\mu\text{m}$, and $N_b = 4 \times 10^9$. For titanium the temperature rise may exceed 1000 K. The table further shows the thermal diffusion length over the bunch train, $l_{\text{diff}} = \sqrt{Kn_b t_b/c_p}$, and the effective rf penetration depth [14], $\delta_e = \Gamma(3/4)\sqrt{2\sigma_z/(c\mu\sigma)}$, where K denotes the thermal conductivity, n_b the number of bunches (154 for CLIC), t_b the bunch spacing (0.67 ns), σ the conductivity and μ the magnetic permeability.

Table 2: Parameters for image current heating.

material	ΔT_1 [K]	l_{diff} [μm]	δ_e [μm]	ΔT_N [K]
Cu	28	3.4	0.06	45
Ti	40	0.85	0.3	1420
W	14	2.9	0.1	131

Fortunately, our above estimates are too pessimistic. If the beam is deflected in the linac to an amplitude where it might impinge on the final-doublet aperture, its emittance at the end of the linac increases dramatically, by several orders of magnitude, as is illustrated in Fig. 1. The emittance growth is explained by rapid filamentation due to the large energy spread. This suggests that typical values of $\sqrt{\beta_x\beta_y}$ found throughout the final focus, *i.e.*, significantly smaller than 1000 km, might still ensure collimator survival for many conceivable failure modes.

The exit line should cleanly remove the spent beam and debris of the beam-beam collision from the interaction region, simultaneously ensuring acceptable background in the detector and not exciting intolerable vibrations of the final-doublet quadrupoles. The outgoing beam has a full energy spread of 100%, and there are copious beamstrahlung photons, carrying a third of the initial beam power, and almost as many coherent pairs as incoming particles [16]. The radial power and energy distribution 2 m from the IP are shown in Fig. 2. The deposition of a small fraction of the full beam power near the final quadrupole could induce elastic waves with amplitudes well in excess of the 0.2 nm vertical jitter tolerance [17, 18]. If we consider a quadrupole a distance of 2 m away from the IP on the outgoing side, and assume that its inner radius is $R = 10$ mm, then, from the average power shown in Fig. 2 (top), the energy deposited in this quadrupole per bunch train is

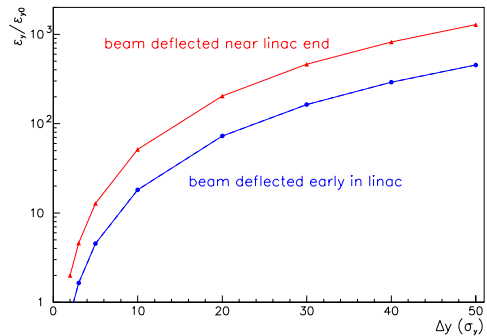


Figure 1: Relative increase in vertical emittance at the end of the linac for a mis-steered beam as a function of oscillation amplitude in units of rms beam size, simulated by the code PLACET [15]. Shown are the results of a bunch deflection after 10% and 90% of the full linac length.

$\Delta E_{\text{train}} \approx 1.6$ J. It will be absorbed in a radial annulus $\Delta R \approx 0.14$ m, *e.g.* of copper. The amplitude of radial elongation is about $\delta R_{\text{train}} \approx \alpha \Delta E_{\text{train}} \Delta R / (C_p V) \approx 1$ nm, where V denotes the volume in which the energy is absorbed. The quadrupole motion induced on the incoming beam line will be much smaller and negligible.

On the other hand, the absorption of the full beam power, 11 MW pulsed at 100 Hz, requires some care. No solid material can stand this power and the thermomechanical vibrations due to beam impact can be orders of magnitude above the final-focus stability tolerances [18]. A dump made of water at 4°C, where the density of water reaches a minimum, might suppress the vibrations to an acceptable level.

Neutron generation in the vicinity of the detector is a further concern. In addition, we anticipate the necessity of numerous spent-beam and beamstrahlung diagnostics, *e.g.* for luminosity optimisation, monitoring and stabilisation.

A crossing angle is necessary at CLIC in order to (1) provide sufficient space for the spent beam and collision debris, in particular for the opposite-charge pairs, and (2) suppress the multi-bunch kink instability. The latter requires a full crossing angle [19] $\phi_c \geq \sqrt{D_x n_b} (3D_y)^{1/4} \phi_d \approx 12$ mrad, with $n_b = 154$ the number of bunches; $D_x = 2N_b r_e \sigma_z / (\gamma(\sigma_x + \sigma_y)\sigma_x) = 0.12$, and $D_y = 5.2$. The former favors crossing angles larger than 20 mrad.

The disadvantage of the crossing angle is the loss in geometric luminosity, *e.g.*, 14% loss for $\phi_c = 20$ mrad. The luminosity is recovered by crab crossing with dipole-mode rf cavities producing a z -dependent displacement at the IP of $\partial x^*/\partial z = \phi_c/2$ or $\phi_c/2 = R_{12} e V_{\text{max}} k_{\text{rf}} / E$. With $R_{12} \approx 23$ m, an rf voltage of $V_{\text{max}} = 1$ MV is needed at 30 GHz. If the relative phase of crab cavities jitters, the collision will not be head-on. The phase tolerance for a 2% luminosity loss reads [20] $\Delta z \leq 4\sigma_x / (5\phi_c)$ or $\Delta\phi_{\text{rf}} \leq k_{\text{rf}} 4\sigma_x / (5\phi_c) \approx 0.06^\circ$ at 30 GHz. The phase tolerance is proportional to the rf frequency.

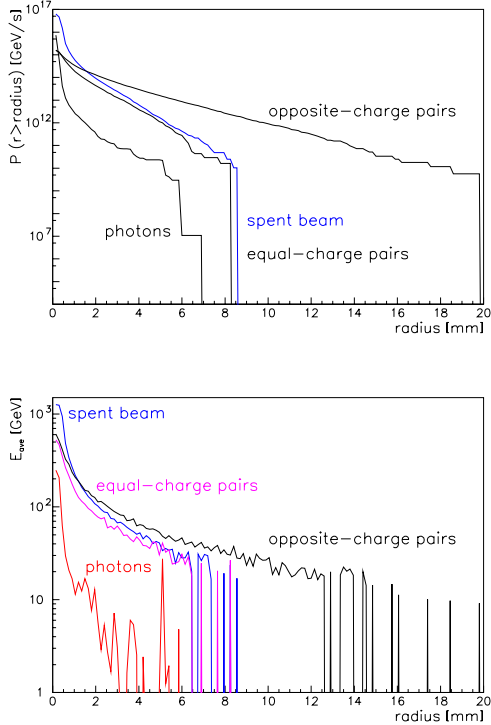


Figure 2: Radial power and energy distribution of debris particles 2 meters away from the IP, as simulated by GUINEA-PIG. Top: integrated power outside radius r vs. r ; bottom: average energy vs. r .

Table 3: Beam parameters required from the damping rings

Normalised emittance	$\gamma\epsilon_x/\gamma\epsilon_y$	430/3 nm
Particles/bunch	N_b	4×10^9
Bunches/train	k_{bt}	154
Bunch spacing	l_b	0.2 m
Rep. rate	f_r	100 Hz

2 DAMPING RINGS

The CLIC damping rings must provide e^+ and e^- beams with the demanding parameters given in Table 3.

The emittances of the beam on injection into the ring determine the storage time in the ring. The positrons will have the larger injected emittances, taken to be $\gamma\epsilon_x = 63 \mu\text{m}$, $\gamma\epsilon_y = 1.5 \mu\text{m}$, as they come from a pre-damping ring.

Although a detailed study has been done for the requirements of a CLIC operating at centre-of-mass energy of 1 TeV [21], the design of the damping rings for 3 TeV is not complete. However a similar parameter optimisation indicates qualitatively similar basic choices for the design of the optics.

The optimum beam energy is around 1.98 GeV and the damping time required in a ring of 380 m circumference is

around 30 ms. As in [21], the ring will have a racetrack shape, with a TME (Theoretical Minimum Emittance [22]) lattice for its arcs and strong wigglers to provide additional damping in the straight sections. The TME optics will be adjusted to balance the need for a small emittance against that for a high momentum compaction to maximise the threshold impedance for turbulent bunch-lengthening.

The energy lost by synchrotron radiation is predominantly in the wiggler sections and these are likely to present the major difficulties for the final design. In order to avoid unwanted emittance generation due to the build-up of the dispersion functions in each wiggler period, the period must be reduced to a few cm. This raises issues related to tolerances on alignment and field quality in the wigglers.

Given the small beams in the ring also intra-beam scattering will contribute to the final emittance. In addition, fast beam-ion instability, single-bunch beam break up driven by the electron-cloud, coherent synchrotron radiation, and space charge effects need to be addressed.

Finally, there may exist a diffractive quantum limit on the IP spot size [23], given by $\sigma_y > \hbar c f / (E \delta_0)$ with $f \approx 5 \text{ m}$ the final focal length and E the energy. Via $\delta_0 \equiv \sqrt{\hbar / (eB)}$ this is related to the wiggler field B in the damping rings. For 3-TeV CLIC parameters and $B \approx 1.5 \text{ T}$, the above limit is $\sigma_y \approx 0.03 \text{ nm}$, a factor of 30 below our design goal.

3 SUMMARY

Conservative design approaches for beam delivery and damping rings have been described, which are based on moderate extensions of proven strategies, adapted to the specific requirements of CLIC at 3 TeV c.m. energy.

REFERENCES

- [1] F. Zimmermann, *et al.*, these proceedings.
- [2] P. Raimondi, private communication (2000).
- [3] S. Fartoukh and J.B. Jeanneret, these proceedings.
- [4] R. Assmann, *et al.*, these proceedings.
- [5] O. Napoly, unpublished.
- [6] R. Brinkmann, private communication (1999).
- [7] H. Burkhardt, CERN-SL-057-AP and CLIC Note 416 (1999).
- [8] R. Brinkmann, talk at LC99, Frascati (1999).
- [9] R. Settles, private communication (2000).
- [10] N. Akasaka *et al.*, "JLC Design Study", KEK (1997).
- [11] R. Brinkmann and N. Walker, LC99, Frascati (1999).
- [12] R. Brinkmann, *et al.*, TESLA 95-25 (1995).
- [13] F. Caspers, private communication (1999).
- [14] X.E. Lin and D.H. Whittum, SLAC-PUB-8393 (2000).
- [15] D. Schulte, these proceedings.
- [16] D. Schulte, PAC99, New York (1999).
- [17] O. Napoly, CLIC note 414 (1999).
- [18] J.B. Jeanneret and E. Wildner, CERN-SL-99-072 (AP) and CLIC Note 42 (1999).
- [19] K. Yokoya, P. Chen, USPAS Hilton Head Island (1990).
- [20] NLC ZDR, SLAC Report 474 (1996).
- [21] J.-P. Potier, T. Risselada, these proceedings.
- [22] L. Teng, FNAL TM-1269 (1984).
- [23] C. Hill, FNAL preprint, subm. to Phys. Rev. D (2000).